Pacific Symposium on Biocomputing 15:190-199(2010)

THE STEADY STATES AND DYNAMICS OF UROKINASE-MEDIATED PLASMIN ACTIVATION

LAKSHMI VENKATRAMAN[1, 2], HANRY YU [2, 3], SOURAV S. BHOWMICK[1, 2], C. FORBES DEWEY JR.[2, 4], LISA TUCKER-KELLOGG[2, 5, *]

[1]*School of Computer Engineering, Nanyang Technological University, Singapore*
[2]*Singapore-MIT Alliance, E4-04-10, 4 Engineering Drive 3, Singapore 117576*
[3]*Department of Physiology, National University of Singapore, Singapore*
[4]*Department of Mechanical Engineering, M.I.T, Cambridge, MA 02130*
[5]*Department of Computer Science, National University of Singapore, Singapore 117417*
** Correspondence to tucker@comp.nus.edu.sg*

Plasmin and urokinase-type plasminogen activator (uPA) are ubiquitous proteases regulating the extracellular environment. They can activate each other via proteolytic cleavage, suggesting the potential for complex dynamic behaviors that could be elucidated by computational modeling. Ordinary differential equations are constructed to model the activation dynamics of plasminogen into plasmin, and single-chain uPA (scUPA) into two-chain uPA (tcUPA). Computational simulations and phase plane analysis reveal two stable steady states for the activation of each protein. Bifurcation analysis shows the *in silico* system to be bistable. Cell-free experiments verify the system to have ultrasensitive activation behavior, where scUPA is the stimulus and plasmin the output. Furthermore, two significantly different steady states could be seen *in vitro* for the same stimulus levels, depending on the initial activation level of the plasmin. The switch-like dynamics of the uPA-plasmin system could have potential relevance to many normal and disease processes including angiogenesis, migration and metastasis, wound healing and fibrosis.

Keywords: Urokinase-Type Plasminogen Activator, Computational modeling, Nonlinear Dynamics

1. INTRODUCTION

Mathematical modeling of molecular interaction kinetics can give insight into dynamic characteristics and time-dependent functions of molecular networks [1-3]. The nonlinearity inherent in such networks can cause dynamical effects that play a transformative role in converting signals into biological functions. Qualitative changes in the outcome of pathway behavior, called bifurcations, arise from nonlinearity of interaction networks and are dependent on the parameter values. Analysis of transitions in system outcome due to changing parameters is called bifurcation analysis [4, 5]. Bifurcation analysis has been used on biological models like the cell-cycle [10, 11]. A common bifurcation in biology is bistability, or existence of two steady states, which transforms a gradual input change into an "all-or-none" switch. Bistability can explain the switch-like nature of apoptosis [6-9] and cell-cycle progression [10-13].

Bistability is most often studied in reversible pathways, especially those involving phosphatases and kinases [14]. Proteases, well known for their importance in the homeostasis of the extracellular matrix (ECM), are enzymes that catalyze the irreversible cleavage of a protein backbone. Some previous work has examined the systems-level dynamics of protease networks [15]. Plasmin (PLS) is a ubiquitous serine protease activated from the secreted protein plasminogen (PLG). Irreversible conversion of PLG to PLS is facilitated by plasminogen activators (PA) which nick at the Arg^{560}-Val^{561} bond of PLG to release the active PLS protease [16]. Tissue Plasminogen Activator (tPA) mediates PLG activation in connective tissues, while urokinase Plasminogen Activator (uPA) mediates PLG activation in the tissue context [17].

PLS is crucial in haemostasis and blood clotting where it converts inactive fibrinogen to fibrin, causing degradation of clots [18]. In tumor angiogenesis, PLS has been confirmed as a pro-angiogenic activator causing dissolution of ECM components to allow for development of new blood tissues [19]. In wound healing, PLS contributes to remodeling of injured/wounded ECM by activating the proteases that dissolve scars [20]. In addition, PLS can activate TGF-β1 from its inactive latent LTGF-β1 form [7, 8, 14] and TGF-β1 is an essential factor in the production of the ECM.

In this paper, we use mathematical modeling to investigate the dynamics of PLS activation by urokinase, and our modeling shows the system to be bistable. The model and its construction are described in Section 2. Simulations and bifurcation analysis of the model follow in Section 3. Finally in Section 4 we show experimental results that validate the mathematical predictions, confirming that uPA-mediated PLS activation is ultrasensitive and bistable.

2. MODEL CONSTRUCTION

Although an integral part of many pathways, proteases have not been as extensively modeled and studied as their kinase-phosphatase counterparts. A protease reaction is generally irreversible, as the cleaved fragments of the substrate diffuse apart and/or the substrate is consumed. Proteases are usually broad-spectrum reactors, meaning they are capable of cleaving different protein substrates having similar target sequences. The simple, classical manner of protease activation is auto-activation (Figure 1a), in which an active protease X cleaves its inactive precursor form. An alternative manner of activation (Figure 1b) operates via regulation of an intermediate regulatory enzyme (Y), which also has active and precursor forms. This is a common type of positive feedback imposed by the activated protease and is seen in pathways such as caspase activation, MMP activation and blood clotting. Figure 1c displays a variant in which the "inactive" precursor Y has some low level of catalytic activity which can by itself initiate activation of the protease.

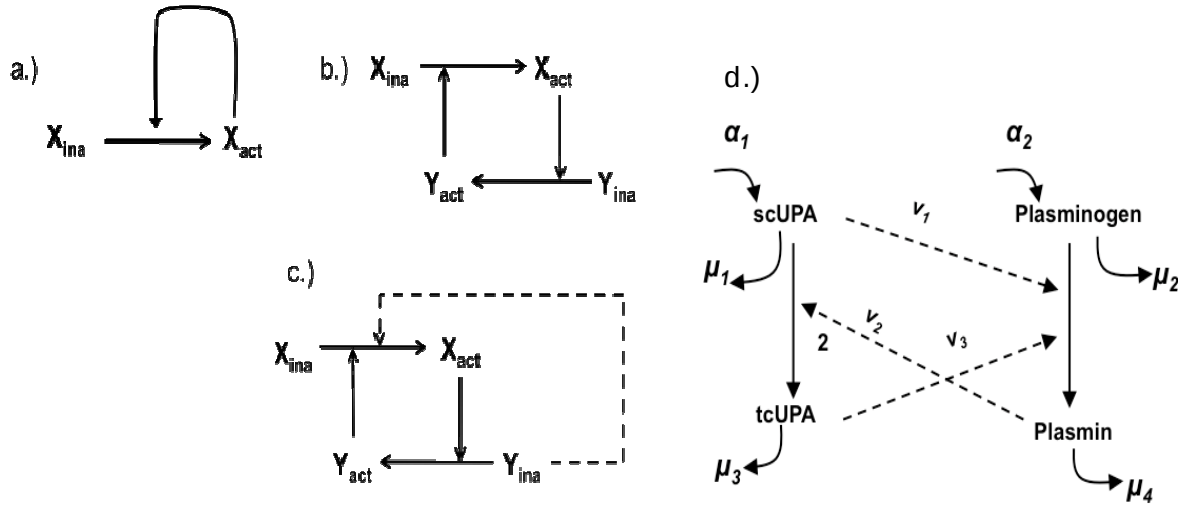

Table 1- Ordinary Differential Equations (ODEs)

ODEs	Reaction Rates
$d[scUPA]/dt=-v_2+\alpha_1-\mu_1*[scUPA]$	$v_1=keff_1*[scUPA]*[PLG]$
$d[PLG]/dt=-v_1-v_3+\alpha_2-\mu_2*[PLG]$	$v_2=keff_2*[scUPA]*[PLS]^n$
$d[PLS]/dt=+v_1+v_3-\mu_4*[PLS]$	$v_3=keff_3*[tcUPA]*[PLG]$
$d[tcUPA]/dt=v_2-\mu_3*[tcUPA]$	

Table 2- Parameter values

Parameters	Values
$keff_1$	0.0017 $\mu M^{-1}min^{-1}$
$keff_2$	1 $\mu M^{-1}min^{-1}$
$keff_3$	0.03 $\mu M^{-1}min^{-1}$
n	3
$\mu_1=\mu_3$	0.0001 min^{-1}
$\mu_2=\mu_4$	0.001 min^{-1}
α_1	0.00009 $\mu M\ min^{-1}$
α_2	0.001 $\mu M\ min^{-1}$

Figure1. Model Construction. a) Active Protease (X_{act}) activating itself from inactive form (X_{ina}). b) Protease feedback through intermediate regulatory enzyme Y. c) Initiator inactive protease (Y_{ina}) activating X. d) Actual model of PLS activation from PLG mediated by uPA. Table 1 showing the ODEs and the reaction rates. μ (1,2,3 and 4) represent degradation of respective species and α (1 and 2) represent production rates of scUPA and PLG respectively. Table 2 lists the normalized parameter values used for modeling.

uPA mediated PLS activation follows the mechanism of Figure 1c with some additional considerations (Figure 1d, and Table 1). UPA is secreted as a single chain form (scUPA) having very little intrinsic activity, but it can cleave the Glu-PLG form of plasminogen to produce PLS[16]. PLS in turn cleaves scUPA into the two-chain form, tcUPA, activating it completely by nicking at the Lys^{158}-Ile^{159} bond. tcUPA has 12-fold greater enzymatic activity for PLG than the scUPA form [16] . tcUPA creates positive feedback (Figure 1d) by cleaving PLG to form more PLS. Being the completely activated form of scUPA, tcUPA has more reactivity to PLG than scUPA. PLS activity has been modeled empirically as a co-operative process with a Hill coefficient (n), similar to reference 21. Substrate competition can be a cause for co-operativity in enzyme action, apart from the traditional mode of allosteric co-operativity [21]. PLS being a broad substrate enzyme could thereby exhibit co-operativity in its activity towards scUPA in the ECM. Production and degradation terms are important in this network (figure 1d) because, for example, if some production process does not occur to balance degradation, then any amount of degradation would eventually cause the system to decay to a single steady state at zero.

Extensive experimental literature on PLS and uPA provides narrow ranges for most rate constants in this model [16, 22-24]. Some parameter uncertainty remains and is examined directly in Sections 3.3 and 3.4. The numerical parameters we chose for closer study, explained in Appendix A and listed in Table 2 of Figure 1, represent a plausible qualitative model, but not an absolute quantification of all phenomena. Our purpose is to use modeling for elucidating possible behaviors, generating hypotheses, and directing experimental design, but we do not draw conclusions from the modeling alone.

3. MODEL SIMULATION

3.1 Steady state behavior of PLS

To understand the behavior of the system, we simulate the PLS-uPA model from Section 2. Using random initial conditions of all the species (Figure 2a), we follow the time progression curves of PLS. Interestingly, we notice that, depending on initial concentrations, PLS can attain two different steady states: a lower steady state at 0.02 μM and a higher one at 0.27μM. Usually reaction systems tend to converge to one steady state, and the presence of two steady states suggests bistability. The steady state behavior of PLS, computed in response to different concentrations of the initiator protease, scUPA, shows a sharp change in PLS steady state levels, caused by very little change in scUPA concentration (between 0.2-0.25 μM, Figure 2b). A system with such high sensitivity to parameter values is called "ultrasensitive" [14].

Since activation is irreversible, we note that turnover would be necessary for the system to be able to switch from activated to inactivated steady states. Indeed, changes in the production rate (which might reasonably occur *in vivo* when different cell types proliferate or die) can cause the system to switch up or down. A time-progression plot (Figure 2c) of PLS, responding to stepwise changes in the scUPA production rate, shows the dependence of PLS steady state on small changes in scUPA production. In this case, scUPA production less than 9.4 μM min^{-1} keeps PLS in its lower steady state; while a production rate of 9.7μM min^{-1} is sufficient to maintain a steady state with higher activation. A variety of other system parameters are capable of causing similar switches in the steady state (not shown).

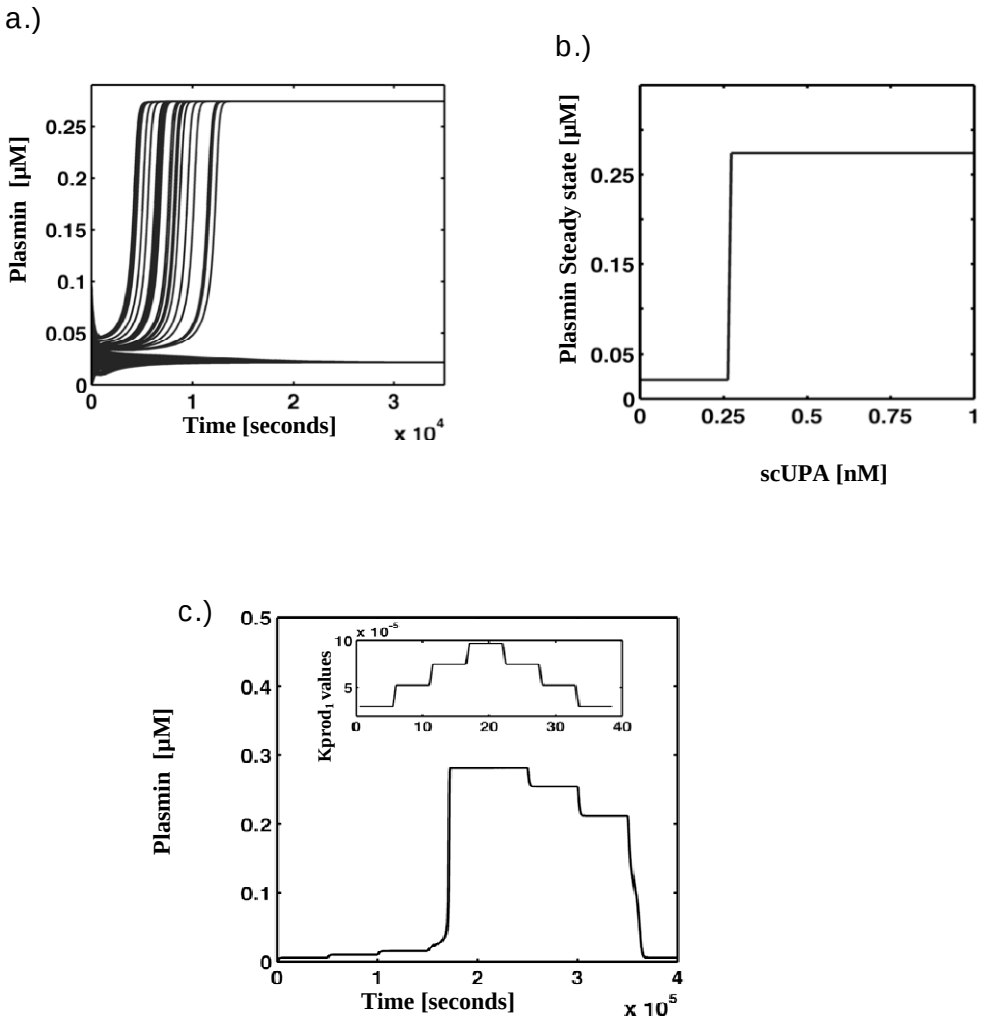

Figure 2. Steady state simulations. a) PLS time progression with random initial concentrations. b) Effect of the production rate of scUPA (α_1) on the time progression of PLS. c) Steady State of PLS for different initial concentrations of scUPA.

3.2 Phase plane Analysis

To investigate the steady states of the system, we used phase plane analysis which projects the full model onto 2 variables, for visualizing the essential dynamics of a minimized representative system. The reduction of the system, shown fully in Appendix B, decreases the number of degrees of freedom in the system by assuming some quantities to have zero derivative, as if at steady state. The sets of points where the remaining species are also at steady state are called *nullclines.* Intersections of nullclines are fixed points (equilibrium points) of the overall system. After the model reduction of Appendix B, the nullclines of the system are as follows:

$$pls\_n = \frac{a * TP}{D_2 + a} \quad (1)$$

$$tcupa\_n = \frac{(pls)^n * keff_2 * TU}{keff_2 * (pls)^n + D_1} \quad (2)$$

The nullclines are plotted in Figure 3, where the tcUPA nullcline is a dotted light grey, and PLS is a solid line. These intersect at three points labeled **A**, **B** and **C**. The solutions of the ODEs are plotted as tiny arrows across the plane, pointing in the direction of time evolution. The trajectory arrows converge towards points **A** and **B,** indicating that **A** and **B** are stable states. **C** is an unstable steady state because trajectories near **C** move the system either towards **A** or **B.** Eigen-value analysis confirms the stability, as points **A** and **B** have real negative Eigen-values while point **C** has positive Eigen-values. The system therefore exhibits two steady states and is "bistable."

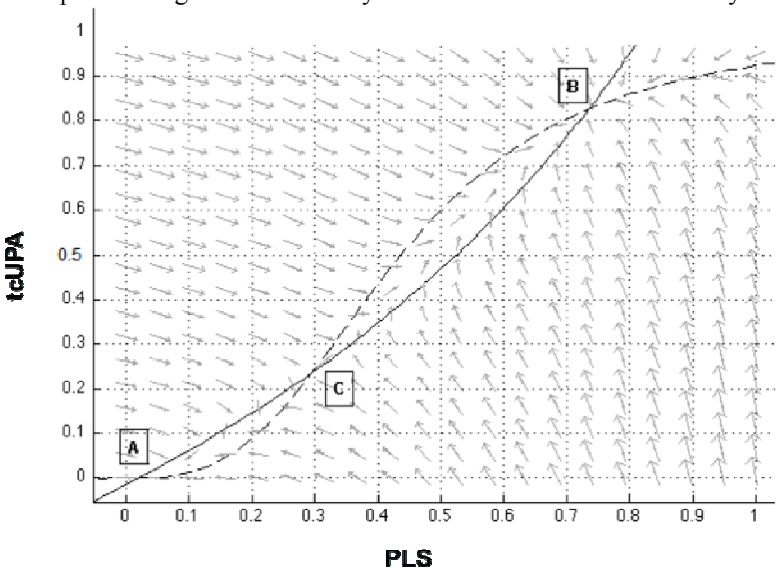

Figure 3: Nullclines for the two species tcUPA (dotted line) and PLS (solid line). The points where nullclines intersect are the steady states of the system. A and B are stable steady states, while C is unstable. Trajectories are shown as smaller arrows

3.3 Bifurcation analysis

The steady state behavior of the model seen in Sections 3.1 and 3.2 is dependent on parameter values. In order to understand how PLS makes the transition from the lower steady state to a higher one, we did bifurcation analysis. Bifurcation analysis relates parameter change with the system response. Figure 4a shows the effect on PLS steady state of changing $Keff_2$, the PLS efficiency parameter. Values of $Keff_2$ between 0.1-1.3 $\mu M^{-1}min^{-1}$ allow PLS to exist in two different steady states (Figure 4a), depending on initial conditions. Starting from an initial higher PLS concentration (grey curve, "Going Down" of Figure 4a), allows the system to achieve the higher steady state over a wider range of $Keff_2$ values before jumping down at $Keff_2 = 0.1\ \mu M^{-1}min^{-1}$.

Starting the system with a lower initial concentration of PLS (black curve, "Going Up", of Figure 4a), shifts into a higher steady state at a different threshold, 1.3 $\mu M^{-1}min^{-1}$ of $Keff_2$. Such systems exhibiting different thresholds for switching between two different steady states are called "hysteretic"[5]. Figure 4b is a bifurcation diagram with $Keff_3$, the tcUPA efficiency rate, as the bifurcation parameter. For $Keff_3 \leq 0.02\ \mu M^{-1}min^{-1}$, the PLS steady state is low, while at $Keff_3$ values higher than 0.053 $\mu M^{-1}min^{-1}$, PLS reaches the higher steady state. The dotted line in Figure 4b describes unstable equilibrium states, to which the system will not converge. Changes in two parameters $Keff_3$ and μ_2 [a degradation parameter, see Appendix B] yield a two-parameter bifurcation diagram (Figure 4c), where the area within the shaded cusp represents configurations with 3 fixed points or bistability, and the areas outside the cusp represent monostable regions.

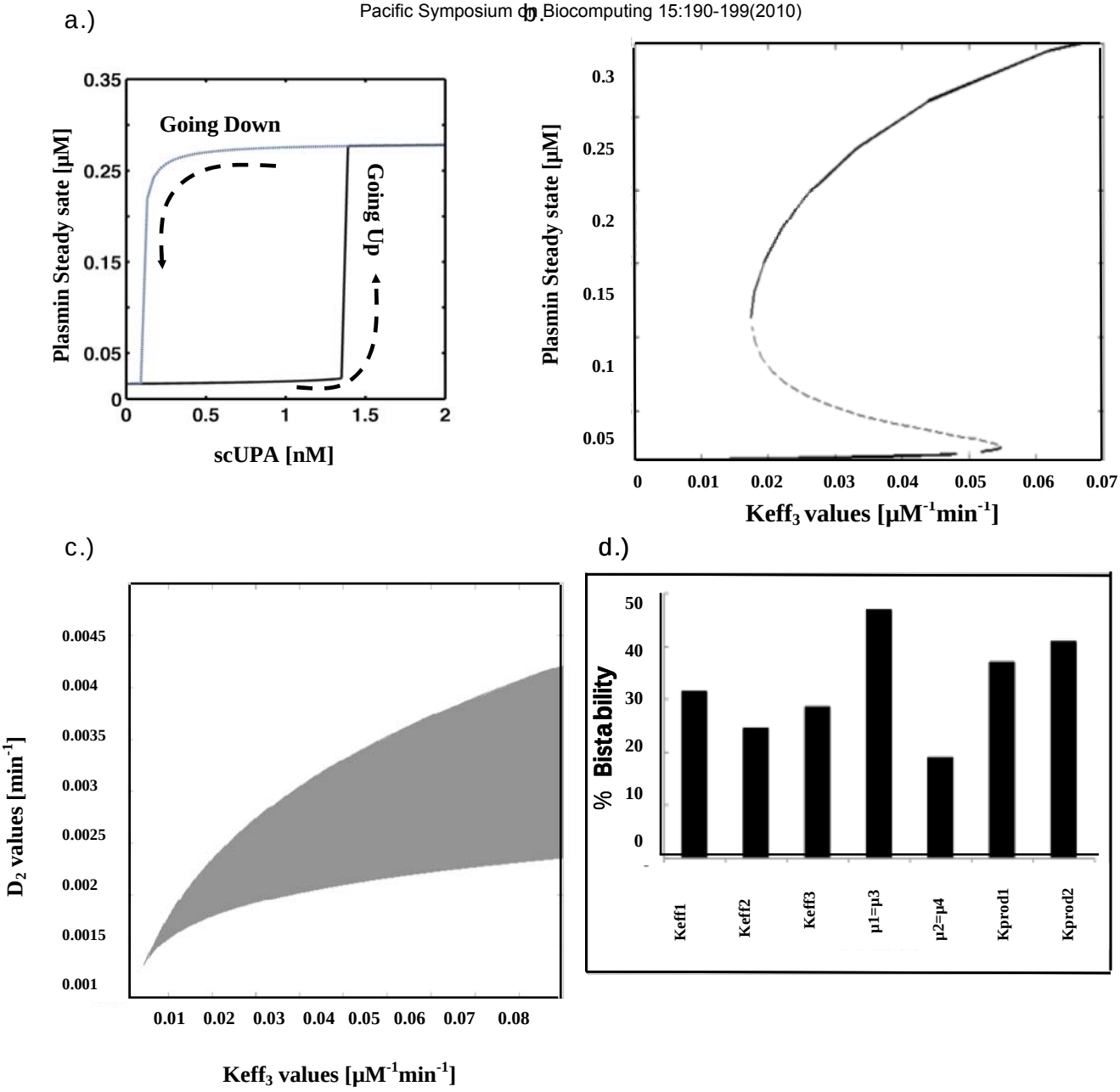

Figure 4: Bifurcation analysis: a) Change in steady state of PLS in μM with change in the $Keff_2$ parameter. b) Bifurcation diagram of PLS with changing the $Keff_3$ parameter. The dashed black line indicates unsteady states. c) 2-Parameter bifurcation diagram with the dark region being bistable. $\mu_2=\mu_3=D_2$. d) Bifurcation parameter robustness.

3.4 Parameter robustness

The bifurcation diagram results indicate a range of parameters over which the system can be bistable. Parameters in a biological system are never known with high confidence, and there are often differences in the same phenomenon between different *in vivo* models. We did a robustness analysis for the presence of bistable behavior in this system over a broad range of all the parameters (20% on either side of reference) [9] and noted the number of parameter sets which are capable of being bistable using a hysteretic technique similar to [25]. Briefly, each parameter was varied +/-20% of its reference value, keeping the other parameters constant, and each was checked for the presence of hysteretic behavior, i.e. a different threshold in the two steady states of the system. As shown in Figure 4d, >=30% of the varied parameter population is still capable of inducing a bistable response in the system.

4. EXPERIMENTAL EVIDENCE

We measured the dynamic behavior of PLS, in an isolated *in-vitro* cell free system. scUPA and PLG are the inputs to the system, which were provided as initial concentrations and also in the form of constant production.

For testing the ultrasensitive nature of the model, we measured PLS steady states after providing different initial concentrations [26]. Variable amounts of scUPA between 0.1nM and 6nM were given, along with a non-variable initial concentration of 1μM PLG. During the progression of the experiments, slight amounts of scUPA and PLG were added, at rates of 50pM/min and 1nM/min, respectively. PLS was monitored using its substrate s-2251, which can be measured as absorbance at 405nm. Figure 5a shows a time profile of PLS activity, which achieves steady state 4 hrs after being initiated with 0.5nM of scUPA. Figure 5b shows the steady state levels of PLS activity in response to variable initial concentrations of scUPA. When initial scUPA levels were 0.9nM or lower, the PLS steady state activity level was low at 0.24 O.D. scUPA levels of 2nM or higher resulted in PLS achieving steady state at a high level (0.95 O.D). Between 0.9 and 2.0nM, the system made a sudden transition in the steady state of PLS. This is a sigmoidal curve, indicative of ultrasensitive behavior, as opposed to a hyperbolic curve typical for Michaelis-Menten reactions [26].

Bistability was verified using the "going-up" and "coming-down" method [27] for observing hysteresis. The "going-up" experiments were initiated with PLS and PLG concentrations in the ratio 60%PLG: 40%PLS (0.6μM PLG: 0.4μM PLS). Varying initial concentrations of scUPA were added, and PLS steady state was monitored. For the "coming-down" experiments, the ratio was reversed (0.4μM PLG: 0.6μM PLS) and parallel values of scUPA were used. Thus we varied the initial activation state of the PLS without varying the absolute amount of the protein. If the system were indeed monostable, then the system would converge to the same steady state of PLS activation, irrespective of the initial activation ratio. As seen in Figure 5c, intermediate concentrations between 0.7nM and 4nM scUPA exhibited two steady states of PLS activation, depending on the initial activation ratio.

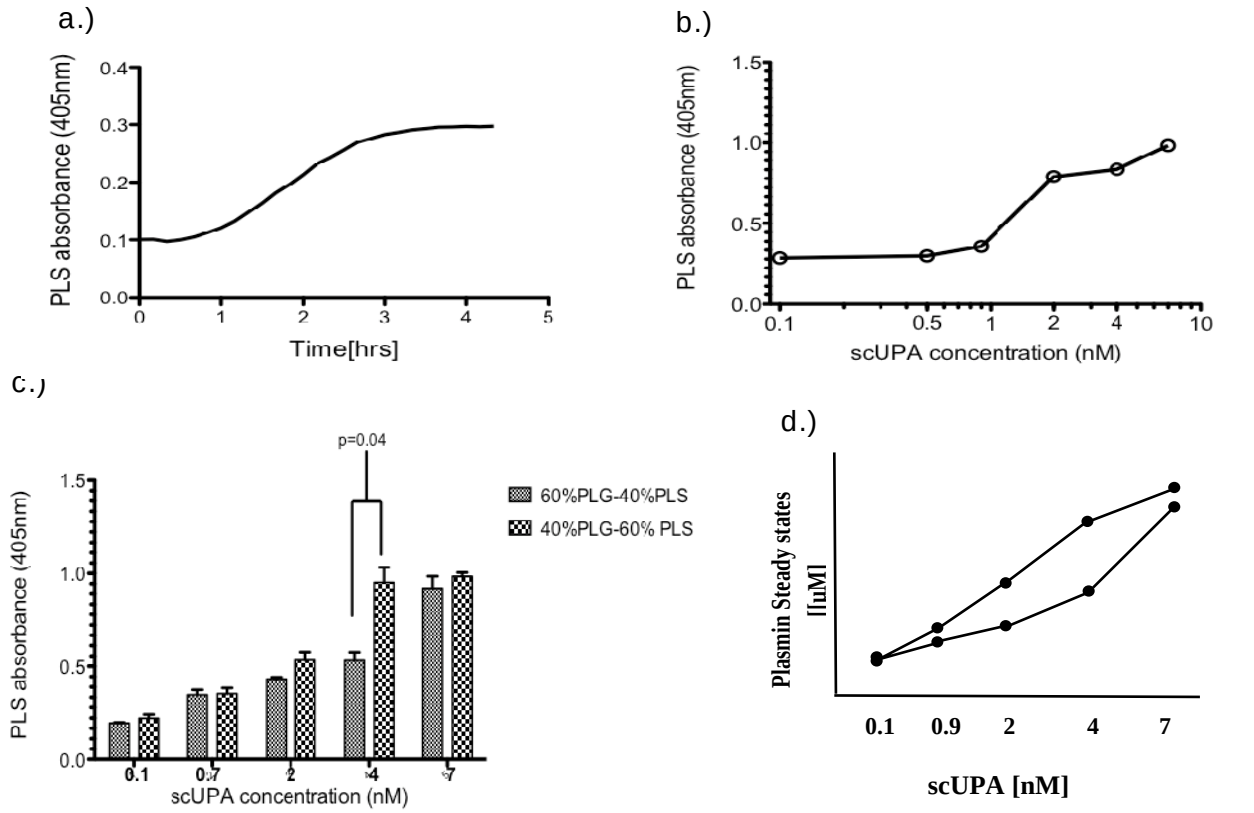

Figure 5-Experimental validation: - a) Time progression curve of PLS achieving steady state after an initial scUPA concentration of 0.5nM .b) Steady state of PLS activity with different scUPA initial concentrations. Steady state levels of PLS activity after initialization with different activation ratios, c) plotted showing the significance of the bistability at 4uM scUPA, and d) plotted in the style of a "going-up" and "coming-down" diagram.

DISCUSSION

In this paper, we employed computational and experimental methods to study the activation behavior of uPA and PLS, a pair of proteases that are crucial to regulating extracellular environments. Our work describes PLS as the system output, but there are significant downstream biological implications for uPA as well, so that uPA activation should also be viewed as an output. Both enzymes are synthesized in relatively inactive forms and both must be cleaved to be activated. They cleave each other in a positive feedback loop, so that any significant accumulation of either enzyme is sufficient to switch both towards their activated forms. Simulations show this arrangement is capable of generating behavior that is bistable as well as ultrasensitive. Simulations also show the importance of turnover. Because degradation causes removal of all forms, but influx affects only the uncleaved forms, the synthesis and degradation rates play an important role in determining the steady state. For example, changes in the production rate are alone sufficient to induce the ultrasensitive change in output (Figure 2b). We verified that the PLS activation dynamics resemble the simulations as follows: small changes in scUPA concentration were capable of causing large absolute increases in PLS activity; and PLS can exhibit two different steady states for the same amount of scUPA protein, depending on the initial activation state of the PLS.

PLS, PLG and urokinase (uPA) are influential in many physiological processes. Our discovery that they can exhibit bistable activation dynamics could have important repercussions for a number of normal and disease processes such as angiogenesis, tumor metastasis, wound healing and fibrosis. Angiogenesis, the process of growing new blood vessels, is tightly regulated by a variety of pro- and anti-angiogenic factors[19]. Angiogenesis occurs as a switch-like decision [28, 29], the mechanism of which is not known. uPA and PLS play crucial roles in angiogenesis [29], and if the PLS-uPA system can exhibit bistable switching, this could contribute to the switch-like behavior of angiogenesis.

Normal cell migration and pathological cell invasion require coordination of proteases and other extracellular factors to remodel the extracellular matrix (ECM). PLS and uPA act directly on the ECM [20], and PLS also regulates many members of the canonical ECM-regulating family, the matrix metalloproteinases (MMPs). The potential of PLS and uPA to switch between two stable levels of activation may have implications for cell migration, such as coordinating diverse, gradual signals into a synchronized cellular function.

Deficiency of uPA or plasminogen has been shown to lead to reduced healing and to promote progression of fibrosis[30]. Fibrosis is often characterized as an overactive wound-healing response [31]. Our observation that uPA and PLS are relatively insensitive to stimuli when they are not near the ultrasensitive threshold might aid in understanding why the wound healing response fails to switch off in some cases. The bistability of the uPA/PLS subsystem may have far-reaching consequences that should be investigated in future work.

MATERIALS AND METHODS

Model simulations were done using the ODE15s stiff solver of MATLAB (www.mathworks.com). Pplane7 was used for Phase plane analysis and XPPAUT (www.math.pitt.edu/~bard/xpp/xpp.html) used for bifurcation analysis.

Human scUPA was purchased from American Diagnostica and Glu-PLG was from Merck. All solutions were prepared in Tris buffer (0.05 M Tris-HCL, 0.10 M NaC1, 0.01% Tween 80, pH 7.4). Chromogenic substrate of PLS, s-2251, with chemical formula H-D-Val-Leu-Lys-pNA.2HCl was purchased from Chromogenix. In the presence of PLS the following reaction occurs, releasing pNA.

H-D-Val-Leu-Lys-pNA + PLS → H-D-Val-Leu-Lys-OH + pNA

The color intensity of pNA can be measured at O.D. of 405nm. A TecanM200 microplate reader was used for measuring changes in absorbance.

ABBREVIATIONS

ECM - Extracellular Matrix; PLG - Plasminogen; PLS - Plasmin; TGF-β1 - Transforming growth factor Beta 1; LTGFβ1 - Latent Transforming growth factor Beta 1;UPA - Urokinase Plasminogen activators; scUPA - single chain Urokinase Plasminogen activator; tcUPA - two chain Urokinase Plasminogen activator; PAI1 - Plasminogen Activator Inhibitor -1;ODE - Ordinary differential equations.

ACKNOWLEDGEMENTS

This work is supported by the Singapore -MIT Alliance Computational and Systems Biology Flagship Project funding to Sourav Bhowmick, Hanry Yu and Forbes Dewey; fellowship and grant R-252-000-342-112 from the Lee Kuan Yew Foundation to Tucker-Kellogg, and by Singapore-MIT Alliance grant C-382-641-004-091 to Tucker-Kellogg.

APPENDIX A

Table 3 –Parameter values and references

Parameters	Parameter values	References	Normalized Values Used (Values/$Keff_2$ *β)
$Keff_1$	0.061 $\mu M^{-1}min^{-1}$	[16]	0.0017 $\mu M^{-1}min^{-1}$
$Keff_2$	35 $\mu M^{-1}min^{-1}$	[8]	1 $\mu M^{-1}min^{-1}$
$Keff_3$	0.978 $\mu M^{-1}min^{-1}$	[16]	0.03 $\mu M^{-1}min^{-1}$
n	1<n<5		3
$\mu_1 = \mu_3$		[32], [6]	0.0001 min^{-1}
$\mu_2=\mu_4$		[33, 34]	0.001 min^{-}
α_1		[35]	0.00009 μM min^{-1}
α_2		[35]	0.001 μM min^{-1}

Table 3 lists the parameter values with references and their normalized values. Although these parameters are consistent with data and highly plausible, they are not necessarily unique. Due to the irreversibility of most of the reactions, production and degradation terms are non-trivial. Degradation (μ_i) and production (α_i) terms have been adjusted based on [32, 35], and they may contain some bias towards values exhibiting bistable behavior. The assumption of equal degradation rates for inactive and active proteases was made for nullclines, similarly to [15]. To avoid numerical errors from the XPPAUT software, the parameters were normalized as follows: all parameter values were divided by $Keff_2$ for rescaling, and multiplied by β for restoring units. β is $1\mu M^{-1}min^{-1}$.

APPENDIX B: REDUCTION METHOD FOR BIFURCATION ANALYSIS

We let TU, the total Urokinase, be defined as scUPA + tcUPA, and TP be defined as PLG + PLS. For analyzing the equilibrium of the system, we assume the following time derivatives to be zero, which would occur if the system is at steady state.

$$TU' = scupa' + tcupa' = 0 \qquad \text{(B.1)}$$

$$TP' = plg' + pls' = 0 \qquad \text{(B.2)}$$

For ease of notation, we assume equal degradation rates of the proteases, $\mu_1=\mu_4=D_1$ and $\mu_2=\mu_3=D_2$. By solving the ODEs at steady state and substituting in (B.1) and (B.2) we get

$$TU' = kprod_1 - D_1(tcupa + scupa) \quad \text{(B.3)}$$

$$TP' = kprod_2 - D_2(pls + plg) \quad \text{(B.4)}$$

Solving (B.3) and (B.5) further at steady state gives

$$TU = \frac{kprod_1}{D_1} = scupa + tcupa \quad \text{(B.5)}$$

$$TP = \frac{kprod_2}{D_2} = plg + pls \quad \text{(B.6)}$$

Substituting PLG=TP-PLS into the ode for PLS and solving for PLS at steady state, we get the PLS nullcine (PLS_n) as

$$pls\_n = \frac{a * TP}{D_2 + a} \quad \text{(B.7)}$$

Where $a = (keff_1 * scupa + keff_3 * tcupa)$ Similarly, the tcUPA nullcline (tcUPA_n) is

$$tcupa\_n = \frac{(pls)^n * keff_2 * TU}{keff_2 * (pls)^n + D_1} \quad \text{(B.8)}$$

REFFERENCES

[1] D. Angeli, Syst Biol (Stevenage) 153 (2006) 61-69.
[2] J.M.B. Bree B. Aldridge, Douglas A. Lauffenburger and Peter K. Sorger, Nat Cell Biol 8 (2006) 1195.
[3] U.S. Bhalla, R. Iyengar, Science 283 (1999) 381-387.
[4] E.M. C. Fall , J Wagner, John Tyson Computational Cell Biology, 2004.
[5] S.H. Strogatz, Nonlinear Dynamics and Chaos: With Applications to Physics, Biology, Chemistry and Engineering, 2001.
[6] E.Z. Bagci, Y. Vodovotz, T.R. Billiar, *et al.*, Biophys J 90 (2006) 1546-1559.
[7] S. Legewie, N. Bluthgen, H. Herzel, PLoS Comput Biol 2 (2006) e120.
[8] T. Eissing, S. Waldherr, F. Allgower, *et al.*, Biophys J 92 (2007) 3332-3334.
[9] J. Cui, C. Chen, H. Lu, *et al.*, PLoS ONE 3 (2008) e1469.
[10] A. Ciliberto, B. Novak, J.J. Tyson, Cell Cycle 4 (2005) 488-493.
[11] B. Novak, Z. Pataki, A. Ciliberto, *et al.*, Chaos 11 (2001) 277-286.
[12] B. Novak, J.J. Tyson, B. Gyorffy, *et al.*, Nat Cell Biol 9 (2007) 724-728.
[13] J.J. Tyson, K.C. Chen, B. Novak, Curr Opin Cell Biol 15 (2003) 221-231.
[14] A. Goldbeter, D.E. Koshland, Proc Natl Acad Sci U S A 78 (1981) 6840-6844.
[15] T. Eissing, S. Waldherr, F. Allgower, *et al.*, Biosystems 90 (2007) 591-601.
[16] M.F.S. Vincent Ellis, and Vijay V. Kakkar, J Biol Chem 262 (1987) 14998-15003.
[17] J.H. Chesebro, G. Knatterud, R. Roberts, *et al.*, Circulation 76 (1987) 142-154.
[18] J.M. Stassen, J. Arnout, H. Deckmyn, Curr Med Chem 11 (2004) 2245-2260.
[19] J. Folkman, Journal of Thrombosis and Haemostasis 1 (2003) 1681-1682.
[20] H.R. Lijnen, Thromb Haemost 86 (2001) 324-333.
[21] S.Y. Kim, J.E. Ferrell, Cell 128 (2007) 1133-1145.
[22] H.R. Lijnen, B. Van Hoef, F. De Cock, *et al.*, Blood 73 (1989) 1864-1872.
[23] D. Collen, C. Zamarron, H.R. Lijnen, *et al.*, J Biol Chem 261 (1986) 1259-1266.
[24] H.R. Lijnen, B. Van Hoef, L. Nelles, *et al.*, J Biol Chem 265 (1990) 5232-5236.
[25] C. Chen, J. Cui, H. Lu, *et al.*, Biophys J 92 (2007) 4304-4315.
[26] A. Goldbeter, D.E. Koshland, J Biol Chem (1984).

[27] J.R. Pomerening, E.D. Sontag, J.E. Ferrell, Nat Cell Biol (2003).
[28] D. Ribatti, B. Nico, E. Crivellato, *et al.*, Leukemia (2007).
[29] V.W. van Hinsbergh, M.A. Engelse, P.H. Quax, Arterioscler Thromb Vasc Biol 26 (2006) 716-728.
[30] W.Y. Li, S.S. Chong, E.Y. Huang, *et al.*, Wound Repair Regen 11 (2003) 239-247.
[31] G.K. Michalopoulos, M. DeFrances, Adv Biochem Eng Biotechnol 93 (2005) 101-134.
[32] H.C. T. Eissing, J Biol Chem 279 (2004) 36892–36897.
[33] J. Travis, G.S. Salvesen, Annu Rev Biochem 52 (1983) 655-709.
[34] M. Kohler, S. Sen, C. Miyashita, *et al.*, Thromb Res 62 (1991) 75-81.
[35] E.Z. Bagci, Y. Vodovotz, T.R. Billiar, *et al.*, Bioph J (2006).